Available online at www.sciencedirect.com

ScienceDirect

Physics Procedia 12 (2011) 248–254

Physics Procedia

LiM 2011

# Residual Stresses at Laser Surface Remelting and Additive Manufacturing

A.V. Gusarov*, M. Pavlov, I. Smurov

*Ecole Nationale d'Ingénieurs de Saint-Etienne, DIPI Laboratory, 58 rue Jean Parot, 42023 Saint-Etienne, France*

**Abstract**

A thermo-elastic model for calculation of the residual stresses is proposed and experimentally validated. Residual stresses depend on the shape of the remelted domain but are independent of its size. The maximum tensile residual stresses arise in the remelted region in the scanning direction. The calculated longitudinal tensile stresses are about twice greater than the transversal ones. The model explains formation of two systems of longitudinal and transversal cracks observed in experiments. The residual stresses are proportional to the difference between the ambient and melting temperatures, which justifies the known method to reduce the stresses by preheating.

*Keywords:* laser track; bead; laser cladding; selective laser melting

## 1. Introduction

Contraction of remelted zones at cooling after laser treatment produces considerable tensile stresses responsible for cracking of brittle materials [1-6]. This problem is typical for various kinds of laser processing as welding [1,2], selective laser melting (SLM) [2-4], surface remelting [5] and cladding [6]. The most general technical solution seems to be preheating of the laser-material interaction zone. Thus, preheating reduces cracking at laser welding [1], and SLM [4]. Crack-free laser-remelted layers can be obtained with preheating [7,8]. High laser power applied at laser cladding [6] assured elevated temperature of the whole sample, which gave the same effect as preheating with an additional energy source and allowed fabrication of crack-free small parts. Increasing the time of laser action in laser melting experiments [2] was found to be favourable to reduce cracking. This can also be explained by the increase of the temperature of the whole sample. The possible mechanism of reducing the thermal stresses at preheating is a transform of the material to a plastic state at elevated temperatures [1].

Mathematical models were developed to estimate thermal and residual stresses at laser treatment [9-11]. They take into account temperature distribution in the laser beam/target interaction zone, plastic flow and solid-state phase transitions. Therefore, these models are specific for a given material and a given process, for example, surface laser remelting, laser cladding, and selective laser melting. This complicates analysis of various experimental data by such models.

* Corresponding author. Tel.: +33-477-43-7585; Fax: +33-477-43-8499.
*E-mail address*: gusarov@enise.fr.


doi:10.1016/j.phpro.2011.03.032

The above-mentioned processes of laser surface remelting and additive manufacturing (SLM and laser cladding) are based on laser beam scanning along straight lines forming uniform laser-remelted tracks and beads on the surface. Critical stresses may arise after the first laser scan, so that studying a single track/bead is proposed in this work. The simplest and, at the same time, the most universal thermo-elastic model is applied. This makes the problem of calculating the residual stresses two-dimensional and independent of the temperature field. Only the shape of the base of the remelted cylinder is to be specified. The results given by the thermo-elastic model should be considered as the stresses, which would be formed if the processes of plastic flow and cracking were frozen till the complete cooling of the target. The actual character of plastic deformation and fracture can be estimated based on the obtained distributions of stresses taking into account mechanical properties of the given material. Shrinkage/expansion at solid-state phase transformations can be taken into account by an effective thermal expansion coefficient averaged over the interval from the ambient temperature to the melting one.

## 2. Model

Let laser beam is scanned along X-axis. Then the problem is uniform in this direction. The deformation state in plane (YZ) is specified by the vector field of displacement $\mathbf{u} = (u_y, u_z)$. The strain tensor with components $\varepsilon_{\beta\gamma}$ is

$$\varepsilon_{xx} = \varepsilon_{xy} = \varepsilon_{xz} = 0, \quad \varepsilon_{yy} = \frac{\partial u_y}{\partial y}, \quad \varepsilon_{zz} = \frac{\partial u_z}{\partial z}, \quad \varepsilon_{yz} = \frac{1}{2}\left(\frac{\partial u_y}{\partial z} + \frac{\partial u_z}{\partial y}\right). \tag{1}$$

In the calculation domain distributions of solid, remelted, and gas phases are specified by the phase indicator functions $\phi_s$, $\phi_r$, and $\phi_g$ respectively, which are equal to 1 in the corresponding phase and 0 otherwise. The generalized Hooke's law for the components of the stress tensor $\sigma_{\beta\gamma}$ is written as

$$\sigma_{\beta\beta} = (1-\phi_g)[\lambda\theta + 2\mu\varepsilon_{\beta\beta} + \phi_r 3\alpha K(T_m - T_a)], \quad \sigma_{xy} = \sigma_{xz} = 0, \quad \sigma_{yz} = (1-\phi_g)2\mu\varepsilon_{yz}, \tag{2}$$

where $\beta = x, y, z$, $\lambda$ is Lame's first parameter, $\mu$ the shear modulus, $K$ the bulk modulus, $\alpha$ the linear thermal expansion coefficient, $T_a$ the ambient temperature, $T_m$ the melting point, and $\theta = \varepsilon_{yy} + \varepsilon_{zz}$. The system of force balance equations

$$\frac{\partial \sigma_{yy}}{\partial y} + \frac{\partial \sigma_{yz}}{\partial z} = 0, \quad \frac{\partial \sigma_{zz}}{\partial z} + \frac{\partial \sigma_{yz}}{\partial y} = 0, \tag{3}$$

is numerically solved by a finite-difference method relative the displacement $\mathbf{u}$.

## 3. Results

Calculations are made for quartz glass and alumina with thermoelastic properties shown in Table 1. Figure 1 shows distributions of residual displacements and stresses in a half-space substrate for various geometries of the remelted domain with ((a), (d), and (e)) and without ((b) and (c)) addition of material. The distributions depend on the shape of the remelted domain but are independent of its size, so that the distances are given in arbitrary units. Calculations indicate that the maximum tensile residual stresses arise in the remelted region in the scanning direction (see the first principal stress $\sigma_1$ in Figure 1). The maximum tensile stresses in the transversal direction (see $\sigma_2$ in Figure 1) are approximately twice as low as those in the scanning (longitudinal) direction. They occupy not only the

Table 1. Thermoelastic properties used for calculations

| Material | $SiO_2$ glass | $Al_2O_3$ |
|---|---|---|
| Shear modulus, $\mu$ (GPa) | 31 | 150 |
| Poisson's ratio | 0.17 | 0.22 |
| Linear thermal expansion coefficient, $\alpha$ ($K^{-1}$) | $5.5 \cdot 10^{-7}$ | $8.4 \cdot 10^{-6}$ |
| Melting point, $T_m$ ($^oC$) | 1700 | 2070 |

remelted domain but also the adjacent not-remelted zone of the substrate and are slightly concentrated near the point with coordinates $y = 1$ and $z = 0$ corresponding to the substrate surface at the boundary of the remelted phase. The maximum compressive residual stresses arise in the band of not-remelted material adjacent to the remelted phase (see $\sigma_3$ in Figure 1) and are directed along the remelted/not-remelted interface in the transversal (YZ) plane.

Comparison of Figs. 1 (b) and 1 (c) indicate that in case of surface remelting without addition of material the shape of the melt pool has a very small impact on the maximum tensile residual stresses in the longitudinal direction (see $\sigma_1 = \sigma_{xx}$). The maximum tensile stresses in the transversal direction (see $\sigma_2$) slightly increase when the melt pool becomes shallower. In case of addition of material the part of the bead above the surface has no considerable effect on the stresses below the surface (compare Figure 1 (a) with Figure 1(b) and Figures 1 (d) and (e) with Figure 1 (c)). The tensile stresses in the bead above the substrate surface are typically lower than the stresses in the remelted domain of the substrate.

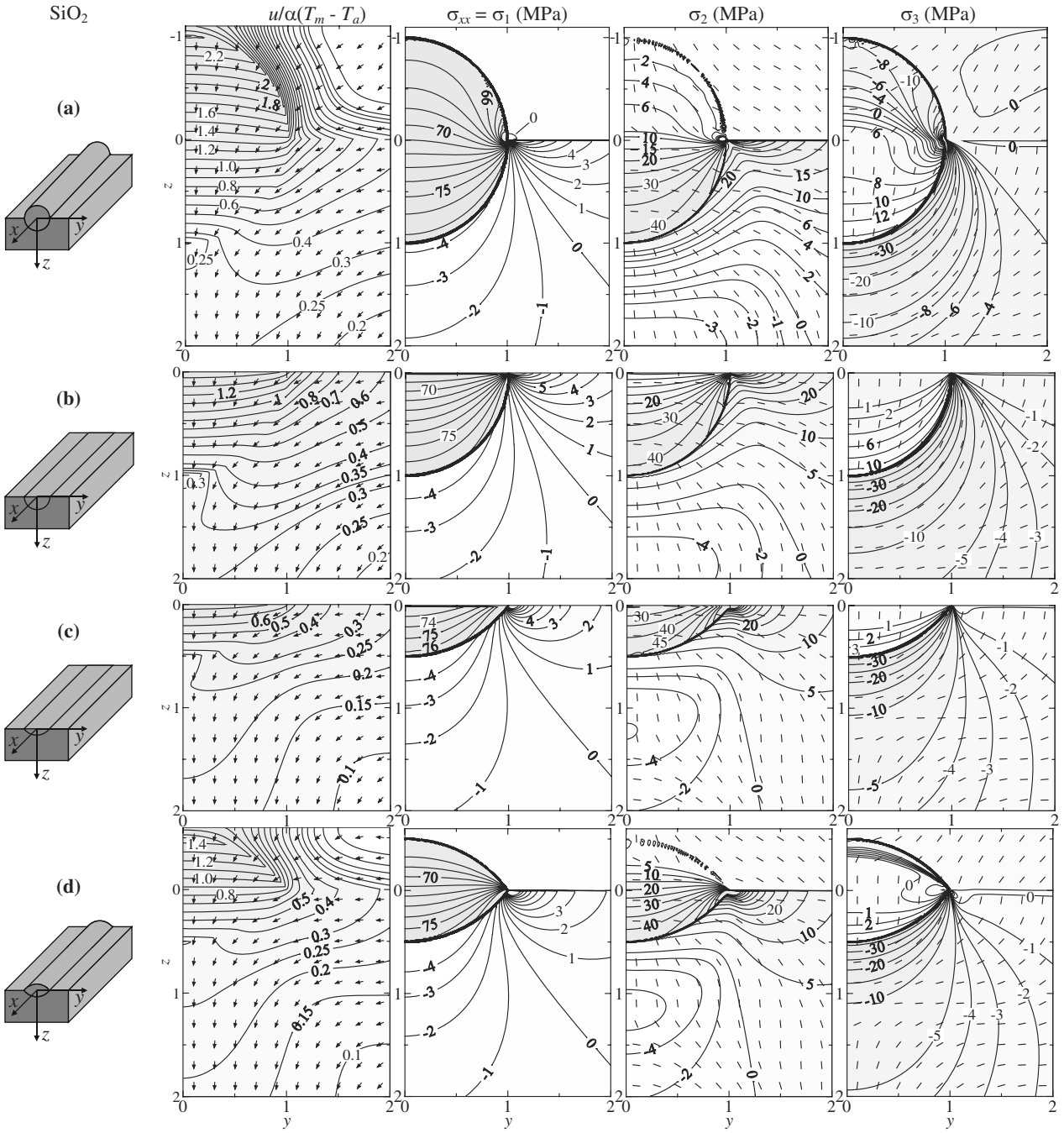


Figure 1. Calculated residual displacement $u$ and principal residual stresses $\sigma_1$, $\sigma_2$, and $\sigma_3$ (MPa) in quartz glass for various profiles of the bead on the surface of a half-infinite body (a)-(e). The absolute value of displacement $u$ is given in the same arbitrary units as $y$ and $z$ coordinates. The displacement direction is shown by arrows. The directions of the principal axes in (YZ) plane are shown by dashes

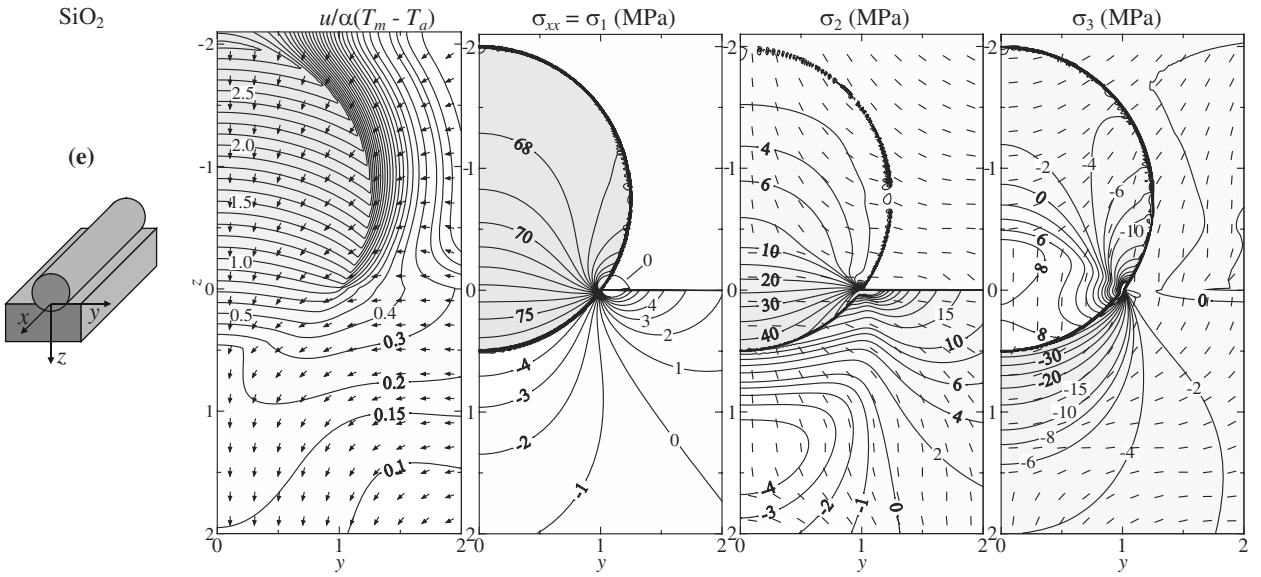


Figure 1. (Continued)

Figure 2 shows the influence of the ambient temperature $T_a$ on the residual stresses at laser remelting of alumina substrate without addition of material. The shape of the remelted domain (Figure 2 (a)) is the same as the shallow melt pool shown in Figure 1 (c). The displacement field (Figure 2 (b)) normalized by the total linear dilatation $\alpha(T_m - T_a)$ is

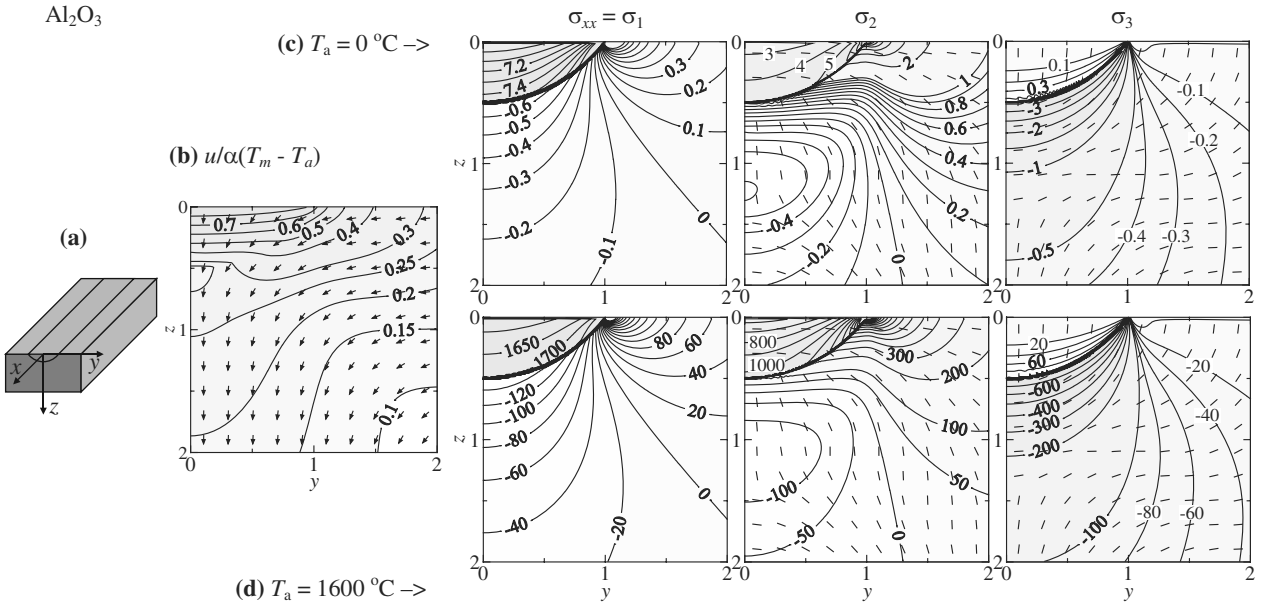


Figure 2. Influence of preheating on residual stresses in alumina: shape of the bead accepted for calculations (a), normalized residual displacement $u$ (b), and principal stresses $\sigma_1$, $\sigma_2$, and $\sigma_3$ without (c) (GPa) and with (d) (MPa) preheating

independent of the ambient temperature and is very similar to that shown in Figure 1 (c). The difference is determined by the different Poisson's ratio. The dimensional displacement is proportional to the temperature difference $(T_m - T_a)$ and the size of the melt pool. The residual stresses are also proportional to the temperature difference. Thus, their absolute value reduces with the increase of the ambient temperature (compare Figs. 2 (c) and (d)).

## 4. Discussion

The usually accepted tensile strength of quartz glass is about 50 MPa. As shown in Figure 1, only the first principal stress slightly exceeds this value. Therefore, formation of cracks in the remelted zone perpendicular to the laser scanning direction is expected in the remelted zone. Nevertheless, cracking was not experimentally observed (see Figure 3). This can be explained by increasing the tensile strength of this material relative with the common value due to small space scale or toughening at high cooling rate specific for laser treatment.

In case of materials with higher thermal expansion, formation of two systems of longitudinal and transverse cracks is often observed as shown in Figure 4, which can be explained as follows. Tensile stresses in the longitudinal direction $\sigma_1$ are about twice greater than the maximum tensile stresses in the transversal direction $\sigma_2$. It is expected that first transversal cracks are formed. This considerably reduces the longitudinal stress and the transverse stress $\sigma_2$ becomes the maximum one. If $\sigma_2$ still exceeds the tensile strength, longitudinal cracks are formed. Tensile stresses in the vertical direction $\sigma_3$ are rather low. Therefore, horizontal cracks were not observed.

Hydroxyapatite shown in Figure 4 (a) is characterized by a very high thermal shrinkage, which allows to evaluate the longitudinal shrinkage as the ratio of the transversal crack width to the average distance between transversal cracks and the transversal shrinkage as the longitudinal crack width to the track width. The longitudinal shrinkage is about twice as high as the transversal one. This is consistent with the same calculated ratio between the longitudinal and transversal stresses.

According to model equations (1)-(3), tresidual stresses are proportional to the difference between the ambient and melting temperatures ($T_m - T_a$). This explains the known method to reduce the stresses by preheating [4,7,8,11].

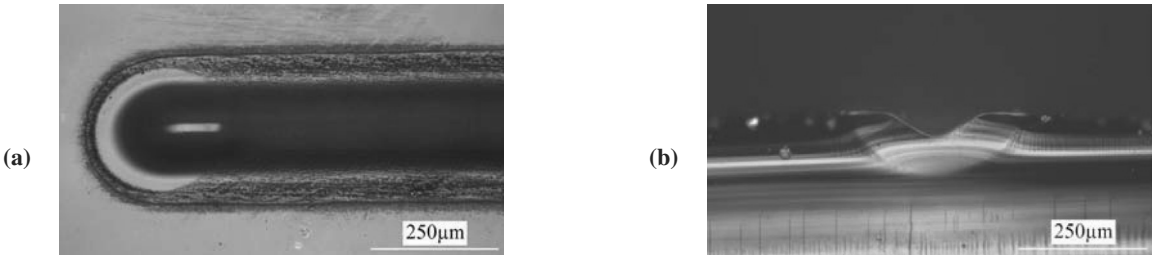


Figure 3. $CO_2$ laser remelting of quartz glass at 12 W laser power, 2 mm/s scanning speed, and 220 μm laser spot diameter: top view (a) and transversal section (b)

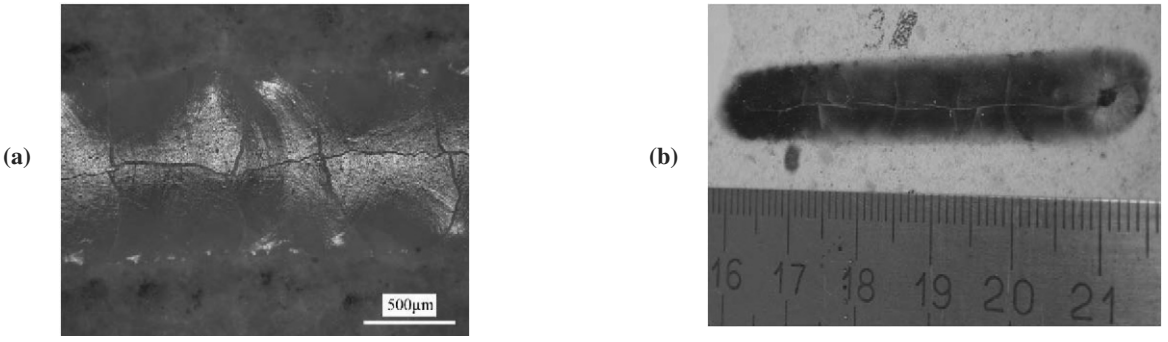


Figure 4. Top views of $CO_2$ laser tracks: (a), hydroxyapatite, laser power 18 W, scanning speed 1 mm/s, laser spot diameter 220 μm; (b), alumosilicate ceramics, laser power 400 W, scanning speed 0.2 mm/s, laser spot diameter 12 mm

This, preheating of the laser processing zone up to 1600 $^{o}$C at SLM of alumina [4] considerably reduced cracking of the obtained parts. Our calculations for this material shown in Figure 2 give the maximum tensile stress of about 7 GPa in the case without preheating (see Figure 2 (c)). Taking into account the value of the tensile strength of alumina of about 300 GPa, cracking should be unavoidable. Notice that according to the accepted model the maximum tensile stress is independent of the space scale of the laser track and very slightly dependent on its shape

(compare Figs. 1 (a)-(e)).

On the contrary, increasing the ambient temperature is a very effective method to reduce the residual stresses. For example, the maximum tensile stress in alumina reduces down to about 1.7 GPa at 1600 $^{o}$C according to Figure 2 (d). Notice that uniform cooling of the final part from the preheating temperature down to the room one doesn't produce additional stresses. The calculated value of tensile stress at preheating is still greater than the tensile strength of alumina. However, a considerable decrease of the width of the cracks is expected. This can be very promising for their elimination by a thermal post-treatment. Cracking can also be reduced due to possible increase of the tensile strength in the conditions of laser treatment as observed for quartz glass or turning the material to the plastic state at elevated temperatures [1].

## 5. Conclusion

According to the proposed model residual stresses depend on the shape of the remelted domain but are independent of its size. The maximum tensile residual stresses arise in the remelted region in the scanning direction. The maximum tensile stresses in the transversal direction are approximately twice as low as those in the scanning direction. This is experimentally validated. The shape of the remelted laser track has a very small impact on the maximum tensile residual stresses. The model explains formation of two systems of longitudinal and transversal cracks observed in experiments. The residual stresses are proportional to the difference between the ambient and melting temperatures, which justifies the known method to reduce the stresses by preheating.

## References

[1] Maruo, H.; Miyamoto, I.; Inoue, Y.; Arata, Y.: $CO_2$ laser welding of ceramics (Report 1). J. Japan Welding Society, 51 (1982), 182-189
[2] Glasser, F. P.; Xiping Jing: Laser melting of refractory $Al_2O_3$-$ZrO_2$ ceramics. British. Ceram. Trans. J., 91 (1992), 195-198
[3] Wilkes, J.; Wissenbach, K.: Rapid manufacturing of ceramic components by selective laser melting. In: Proc. LIM (2007), 207-211
[4] Hagedorn, Y.-C.; Wilkes, J.; Meiners, W.; Wissenbach, K.; Poprawe, R.: Net shaped high performance oxide ceramic parts by selective laser melting. Phys. Procedia, 5 (2010), 587-594
[5] Bacciochini, A.; Glandut, N.; Lefort, P.: Surface densification of porous ZrC by a laser process. J. Europ. Ceram. Soc., 29 (2009), 1507-11
[6] Comesana, R.; Lusquinos, F.; del Val, J.; Malot, T.; López-Álvarez, M.; Riveiro, A.; Quintero, F. ; Boutinguiza, M.; Aubry, P.; De Carlos, A.; Pou, J.: Calcium phosphate grafts produced by rapid prototyping based on laser cladding. J. Europ. Ceram. Soc., 31 (2011) 29-41
[7] Ester, F. J.; Larrea, A.; Merino, R. I.: Processing and microstructural study of surface laser remelted $Al_2O_3$–YSZ–YAG eutectic plates. J. Europ. Ceram. Soc. (2010), doi: 10.1016/j.jeurceramsoc.2010.08.016
[8] Gurauskis, J.; Lennikov, V.; de la Fuente, G. F.; Merino, R. I.: Laser-assisted, crack-free surface melting of large eutectic ceramic bodies. J. Europ. Ceram. Soc. (2010), doi: 10.1016/j.jeurceramsoc.2010.08.017
[9] Ghosh, S.; Choi, J.: Modeling and experimental verification of transient/residual stresses and microstructure formation in multi-layer laser aided DMD process. J. Heat Transfer, 128 (2006), 662-679
[10] Brückner, F.; Lepski, D.; Beyer, E.: Modeling the influence of process parameters and additional heat sources on residual stresses in laser cladding. J. Thermal Spray Technology, 16 (2007), 355-373.
[11] Brückner, F.; Lepski, D.; Beyer, E.: Calculation of stresses in two- and three-dimensional structures generated by induction assisted laser cladding. In: Proc. LIM (2009), 115-120